AIP Advances CELEBRATING 5 YEARS

Analysis of the transient response of nuclear spins in GaAs with/without nuclear magnetic resonance

Mahmoud Rasly, Zhichao Lin, Masafumi Yamamoto, and Tetsuya Uemura

Citation: AIP Advances **6**, 056305 (2016); doi: 10.1063/1.4943610
View online: http://dx.doi.org/10.1063/1.4943610
View Table of Contents: http://scitation.aip.org/content/aip/journal/adva/6/5?ver=pdfcov
Published by the AIP Publishing

AIP ADVANCES **6**, 056305 (2016)

Analysis of the transient response of nuclear spins in GaAs with/without nuclear magnetic resonance

Mahmoud Rasly, Zhichao Lin, Masafumi Yamamoto, and Tetsuya Uemura[a]
Graduate School of Information Science and Technology, Hokkaido Univ., Sapporo 060-0814, Japan

(Presented 13 January 2016; received 6 November 2015; accepted 28 December 2015; published online 4 March 2016)

As an alternative to studying the steady-state responses of nuclear spins in solid state systems, working within a transient-state framework can reveal interesting phenomena. The response of nuclear spins in GaAs to a changing magnetic field was analyzed based on the time evolution of nuclear spin temperature. Simulation results well reproduced our experimental results for the transient oblique Hanle signals observed in an all-electrical spin injection device. The analysis showed that the so called dynamic nuclear polarization can be treated as a cooling tool for the nuclear spins: It works as a provider to exchange spin angular momentum between polarized electron spins and nuclear spins through the hyperfine interaction, leading to an increase in the nuclear polarization. In addition, a time-delay of the nuclear spin temperature with a fast sweep of the external magnetic field produces a possible transient state for the nuclear spin polarization. On the other hand, the nuclear magnetic resonance acts as a heating tool for a nuclear spin system. This causes the nuclear spin temperature to jump to infinity: i.e., the average nuclear spins along with the nuclear field vanish at resonant fields of ^{75}As, ^{69}Ga and ^{71}Ga, showing an interesting step-dip structure in the oblique Hanle signals. These analyses provide a quantitative understanding of nuclear spin dynamics in semiconductors for application in future computation processing. [http://dx.doi.org/10.1063/1.4943610]

I. INTRODUCTION

Controlling the nuclear spins in a semiconductor through nuclear magnetic resonance (NMR) is one of the promising tools for implementing quantum bits (qubits) for quantum computation applications because they have an extremely longer coherence time than electrons. However, the magnetic moment of a nuclear spin is three orders of magnitude smaller than that of an electron spin, so the control of nuclear spins at the nanoscale level is a field of interest.[1] From this point of view, researchers developed dynamic nuclear polarization (DNP) as a way to enhance the NMR signal. In the DNP process spin angular momentum is efficiently exchanged between electron spins and nuclear spins through the hyperfine interaction. For instance, nuclear spins are electrically polarized using a flow of spin-polarized electrons injected from a highly polarized spin source, such as a Heusler alloy, into a semiconductor channel, through a technique called spin injection. A great deal of interest has been expressed towards improving DNP in semiconductors[2–17] and we have successfully developed a strong platform for work in this field.[1,18–24]

Nuclear spins are coupled to each other by spin-spin interactions, and also loosely coupled to a lattice by a spin-lattice relaxation mechanism. The lattice acts as a thermostat for the spin system. Once the thermal equilibrium between the two systems has been established for a given value of the static magnetic field and prior to the application of an rf field, a temperature equal to that of the

[a]Corresponding author: uemura@ist.hokudai.ac.jp

lattice can be assigned to the spins. This means that the macroscopic properties of the spin system can obey the Boltzmann distribution. However, the nuclear spin system is isolated from the lattice owing to a long spin-lattice relaxation time T_1 (~seconds to hours). The interactions inside the nuclear spin system (dipole-dipole interaction of the nuclear magnetic moments) are characterized by much shorter time. Each of the nuclei experiences a fluctuating local field B_L created by its neighbors. This field is typically a few Gauss. The period of the nuclear spin precession in B_L, which is of the order of 10^{-4} s, defines the characteristic time of interaction T_2 in the nuclear spin system. Because of these internal interactions, the nuclear spin system reaches the internal thermodynamic equilibrium during a time of order T_2. This equilibrium state is defined by a parameter called spin temperature,[25] which may differ strongly from the lattice temperature.

To detect the nuclear Overhauser field, oblique Hanle effect measurements have been widely used.[1,2,12–17] While the electrical detection of oblique Hanle signals had been done only in a steady state where the magnetic field was swept slowly enough to ensure that the nuclear spin polarization was in equilibrium,[14] we recently investigated the transient response of nuclear spins to a change in the magnetic field along with a time scale needed for DNP through transient oblique Hanle effect measurements in an all-electrical spin injection device with a Co_2MnSi spin source, with and without NMR.[1] However, rather complicated behaviors of nuclear spins responses were obtained and only a qualitative understanding for this has been achieved. To fully exploit the nuclear spins in future quantum computation systems, it is necessary to understand all possible states for nuclear spin distributions. Therefore, the object of this study is to quantitatively address the time dependence of transient nuclear spin temperature along with the steady-state one, based on various possible nuclear spin distributions, to a change in a static magnetic field with and without NMR.

II. SIMULATION MODEL

Since the nuclear spin system reaches the thermodynamic equilibrium during the spin-spin relaxation time T_2, which is much shorter than the spin-lattice relaxation time T_1, the nuclear spin system is considered as an isolated system from the lattice. Based on Curie's law, the average nuclear spin $\mathbf{I_{av}}^{(\alpha)}$ and resultant Overhauser field $\mathbf{B_n}$ of all nuclei in the presence of external magnetic field $\mathbf{B_{ob}}$ are given by[26]

$$\mathbf{I}_{av}^{(\alpha)} = \frac{(I_\alpha + 1)\mu_I^{(\alpha)}}{3k_B\theta_\alpha}\boldsymbol{B}_{\mathbf{ob}} \tag{1}$$

$$\mathbf{B_n} = \sum_\alpha b_n^{(\alpha)}\mathbf{I_{av}}^{(\alpha)}/I_\alpha \tag{2}$$

where α denotes nuclei species, I_α is the value of nuclear spin, $\mu_I^{(\alpha)}$ is the nuclear magnetic moment, k_B is the Boltzmann constant, θ_α is the nuclear spin temperature, and $b_n^{(\alpha)}$ is the effective nuclear field at 100% nuclear spin polarization. In the case of GaAs, $b_n^{(\alpha)}$ (α=^{75}As, ^{69}Ga, and ^{71}Ga nuclei) values are negative.[26]

In the presence of polarized electrons, nuclear spins are effectively polarized through the transfer of spin angular momentum from polarized electrons to nuclei, leading to the cooling of the nuclear spin temperature. The sign of the nuclear spin temperature is positive (negative) when the sign of $\mathbf{B_{ob}}\cdot\mathbf{S}$ is positive (negative), where $\mathbf{S}$ is average electron spin ($|\mathbf{S}|$ = ½, corresponding to 100% polarization). In the case that $\mathbf{B_{ob}}\cdot\mathbf{S}$ is positive, the spin angular momentum parallel to $\mathbf{B_{ob}}$ is transferred into the nuclear spin system, leading to an increase in the nuclear spin number in the lower energy level. This corresponds to cooling of the nuclear spin temperature below the lattice temperature (*see* Fig. 1(b)). When $\mathbf{B_{ob}}\cdot\mathbf{S}$ is negative, on the other hand, nuclear spins are negatively polarized because a population inversion happens through the transfer of spin angular momentum antiparallel to $\mathbf{B_{ob}}$, and nuclear spin temperature become negative (*see* Fig. 1(c)). However, this description is for the steady states of nuclear spins. If the external magnetic field is changed faster than the time scale of the DNP, then the transient response of nuclear spins should be considered.

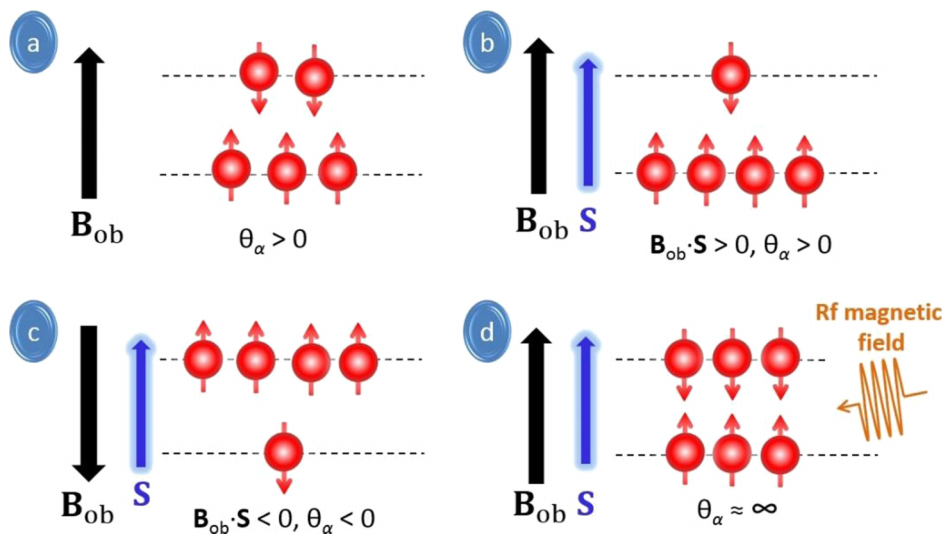

FIG. 1. Schematic description for nuclear spin distribution (a) under an external magnetic field, (b) under the DNP process when $\mathbf{B_{ob}}\cdot\mathbf{S} > 0$, (c) under the DNP process when $\mathbf{B_{ob}}\cdot\mathbf{S} < 0$, (d) at the nuclear magnetic resonance, where $\mathbf{B_{ob}}$ is the oblique magnetic field and $\mathbf{S}$ is the average electron spin.

The first consideration is for the case without irradiation by an rf field; i.e., without an NMR signal. At the energy balance of the nuclear spin system interacting with polarized electrons, the time evolution of nuclear spin temperature under the DNP process is expressed by the following equation:[26]

$$\frac{d}{dt}\left(\frac{1}{\theta_\alpha}\right) = -\frac{1}{T_{1e}}\left(\frac{1}{\theta_\alpha} - \frac{1}{\theta_{0\alpha}}\right) \tag{3}$$

where T_{1e} is the characteristic time for DNP which can be as long as several hundred seconds, and $\theta_{0\alpha}$ is the steady-state nuclear spin temperature, which is given by[26]

$$\frac{1}{k_B\theta_{0\alpha}} = f_\alpha \frac{4I_\alpha}{\mu_I^{(\alpha)}} \frac{\mathbf{B_{ob}}\cdot\mathbf{S}}{\mathbf{B_{ob}^2} + \xi B_L^2} \tag{4}$$

where $f_\alpha(\leq 1)$ is the leakage factor, and ξ is a numerical coefficient which depends on the nature of the spin-spin interactions.

The second consideration is for the case with irradiation by an rf field; when the Zeeman splitting energy of nuclear spins due to a static magnetic field and the energy of an irradiated rf-magnetic field are equivalent, nuclear magnetic resonance (NMR) occurs. This condition is given by[1,17]

$$\gamma_\alpha\,|\mathbf{B_{ob}}| = \omega \tag{5}$$

where γ_α is a gyromagnetic ratio of all nuclei types contained in GaAs and $\omega = 2\pi f_{\mathrm{rf}}$ is the angular frequency of the irradiated rf-magnetic field. For this work, we considered that there are three values for γ_α (6.45, 8.19, and 4.60×10^7 rad/T·s) corresponding to three kinds of nuclei, ^{75}As, ^{69}Ga and ^{71}Ga, respectively in GaAs. At the magnetic resonance of each nucleus; nuclear spins are equally distributed between the energy levels (*see* Fig. 1(d)) because of the absorbed rf energy; i.e., the nuclear spin temperature is going to infinity. Hence, in order to include the NMR effect in our simulation, we reset the reciprocal nuclear spin temperature, θ_α^{-1}, to zero if equation (5) is satisfied.

In electrical oblique Hanle effect measurement using a four-terminal nonlocal geometry in a lateral spin transport device (Fig. 2),[27–29] the Overhauser field can be detected through the detection of nonlocal voltage V_{NL} between contact 3 and 4. Since the easy axis of the ferromagnetic electrodes is along the x-axis direction, we assume that $\mathbf{S_0}$ is also along the x-axis and stays unchanged, where $\mathbf{S_0}$ is average electron spin at $\mathbf{B_{ob}} = \mathbf{0}$. The total magnetic field of $\mathbf{B_{ob}} + \mathbf{B_n}$ induces Hanle precession for electron spins, resulting in a decrease of electron spin polarization under detector contact-3. Similarly to the conventional nonlocal Hanle signal, V_{NL} can be described by[30,31]

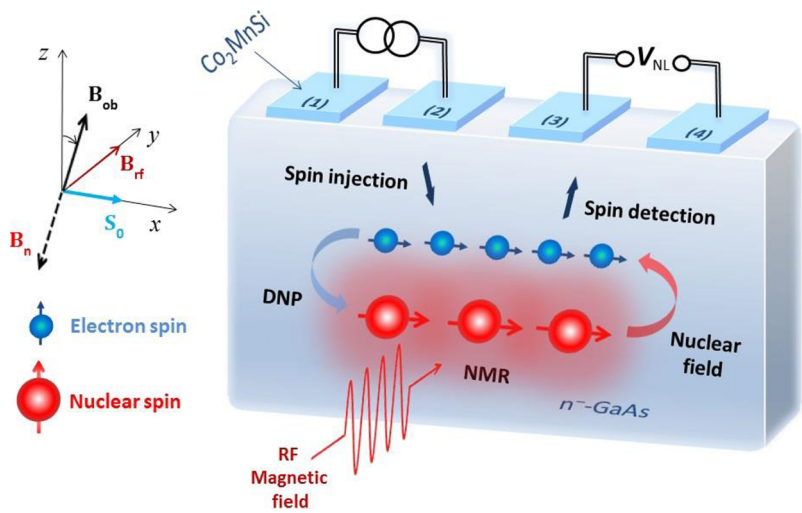

FIG. 2. Schematic structure of a four-terminal non-local device and the circuit configuration used for transient oblique Hanle effect measurements (with/without an rf magnetic field).

$$V_{\mathrm{NL}} = A \int_0^{\infty} \frac{1}{\sqrt{4\pi Dt}} \exp\left(-\frac{d^2}{4Dt}\right) \cos(\omega_L t) \exp\left(-\frac{t}{\tau_s}\right) dt \tag{6}$$

where A is a constant, D is the diffusion constant, d is the distance between contact-2 and contact-3, τ_s is the electron spin relaxation time, and $\omega_L = g\mu_B B_z/\hbar$ is the Larmor frequency where B_z is the z component of $\mathbf{B_{ob}} + \mathbf{B_n}$, g is an electron g-factor ($g = -0.44$ for GaAs), μ_B is the Bohr magneton, and $\hbar$ is the reduced Planck's constant. By using eqs. (1)-(6), we simulated the transient response of nuclear spins against a change in the magnetic field, with/without an rf magnetic field to clarify the dynamics of nuclear spins.

III. RESULTS & DISCUSSION

Figure 3 shows (a) an experimental result of a typical oblique Hanle signal without irradiation by an rf magnetic field (*black curve*) and with irradiation by an rf magnetic field (*red curve*), observed in GaAs with a Co_2MnSi spin source, and (b) a corresponding simulation result obtained using equations (1)-(6). A four-terminal lateral spin transport device (Fig. 2) consists of a 2.5-μm-thick n^--GaAs

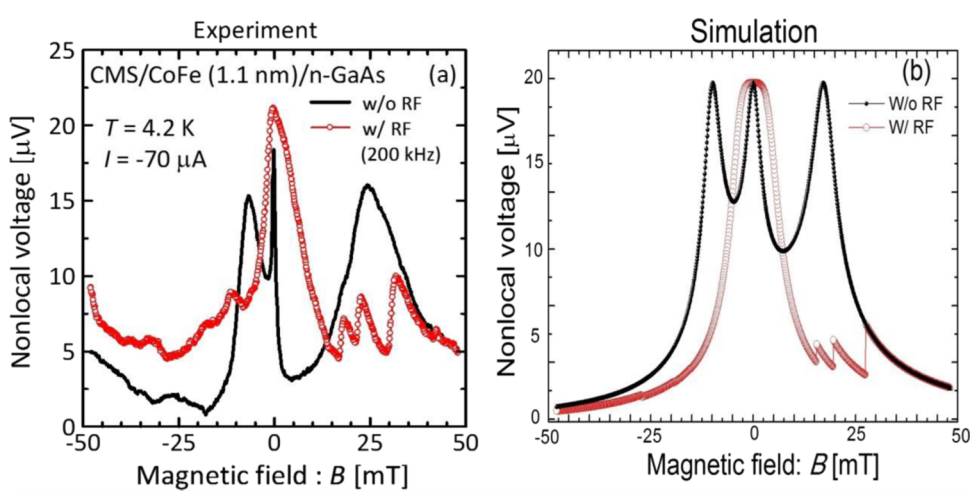

FIG. 3. (a) Transient oblique Hanle signals without (*black curve*) and with (*red curve*) irradiation by an rf magnetic field observed in GaAs with a Co_2MnSi spin source. (b) A corresponding simulation result obtained using equations (1)-(6).

channel with a doping concentration of 3×10^{16} cm^{-3} and a Co_2MnSi(5 nm)/CoFe(1.1 nm) spin source. A 15-nm-thick $n^- \rightarrow n^+$-GaAs transition layer and a 15-nm-thick n^+-GaAs layer with a doping concentration of 5×10^{18} cm^{-3} was inserted between the n^--GaAs channel and CoFe to form a narrow Schottky barrier. The size of the injector contact (contact-2) and detector contact (contact-3) were 0.5 × 10 μm and 1.0 × 10 μm, respectively, and spacing between the contacts was 0.5 μm. The external magnetic field $\mathbf{B_{ob}}$ was obliquely applied at an angle $\varphi = 15°$ from the z-axis in the x-z plane; *i.e.*, $\mathbf{B_{ob}} = B_{ob}(\mathbf{x} \sin\varphi + \mathbf{z} \cos\varphi)$, where B_{ob} is the amplitude of the oblique field of $\mathbf{B_{ob}}$ with both positive and negative signs, and $\mathbf{x}$ and $\mathbf{z}$ are unit vectors along the x-axis and z-axis directions, respectively. The device was first initialized at $B_{ob} = +42$ mT for a hold time (t_{hold}) of 60 s, so that nuclear spins became dynamically polarized. Then B_{ob} was swept from +42 mT to −42 mT with a sweep rate of 0.18 mT/s. The nuclear-spin states were then manipulated through the NMR by irradiation by an rf magnetic field ($\mathbf{B_{rf}}$) along the y-axis direction. The manipulated nuclear-spin states could be read out through detection of the nonlocal voltage (V_{NL}) between contact-3 and contact-4 since the nuclear magnetic field produced by nuclear-spin polarization induces the Larmor precession of electron spins below detector contact-3. The more details of the device structures and experimental conditions are described in references.[1,17]

In the simulation we considered three kinds of nuclei, ^{75}As, ^{69}Ga and ^{71}Ga, in the GaAs channel. Parameters used in our model are listed in Table I. The values of $2|\mathbf{S_0}|$, l_{sf} and τ_{sf} were estimated from fitting of our previous experimental results for spin-valve signals (V_{NL} vs. in-plane magnetic field along the x-axis) and Hanle signals (V_{NL} vs. out-of-plane magnetic field) observed in a lateral spin transport device with Co_2MnSi/CoFe electrodes.[17] The projection of $\mathbf{S}$ to $\mathbf{B_{ob}}$ in eq. (4) was estimated from $|\mathbf{S_0}|$. Although the Hanle precession through $\mathbf{B_{ob}} + \mathbf{B_n}$ changes the component of $\mathbf{S}$ perpendicular to $\mathbf{B_{ob}}$, it does not change the component of $\mathbf{S}$ parallel to $\mathbf{B_{ob}}$. Thus, we assumed that $\mathbf{S}\cdot\mathbf{B_{ob}}$ is equal to $\mathbf{S_0}\cdot\mathbf{B_{ob}}$ in the simulation. The values of $b_n^{(\alpha)}$, T_{1e} and f_α in Table I were treated as fitting parameters. The values of I_α and γ_α were taken from ref. 26 and the value of ξB_L^2 was taken from ref. 14.

Our experimental results for the oblique Hanle effect showed basically two features: (1) Without irradiation by an rf field, an additional side peak at $B_{ob} < 0$ is produced, and (2) with irradiation by an rf field, a step-dip structure in the place of the corresponding peak to nuclear spin polarization is observed. These features are somewhat far from the steady state framework and strongly correlated to the transient response of nuclear spins.[17] The simulation result well reproduced these features. The value of T_{1e}= 650 s used in our simulation is reasonable as a time scale necessary for the DNP.[12,13,17] These results validate the simulation model used in this study. Therefore, in the next two sections we will clarify the origin of these features through an interpretation of the nuclear spin temperature at the steady state and the transient-time evolution of the nuclear spin temperature.

TABLE I. Simulation parameters.

Parameter	Value
$2\|\mathbf{S_0}\|$	4.4 %
l_{sf}	5 μm
b_n of ^{75}As	-3.59 T
b_n of ^{69}Ga	-2.19 T
b_n of ^{71}Ga	-1.99 T
γ_α of ^{75}As	4.581×10^7 rad/T·s [26]
γ_α of ^{69}Ga	6.420×10^7 rad/T·s [26]
γ_α of ^{71}Ga	8.158×10^7 rad/T·s [26]
T_{1e}	650 sec
f_α	0.85
I_α	3/2 [26]
ξB_L^2	5 mT [14]
D	0.5 μm
τ_s	20 ns

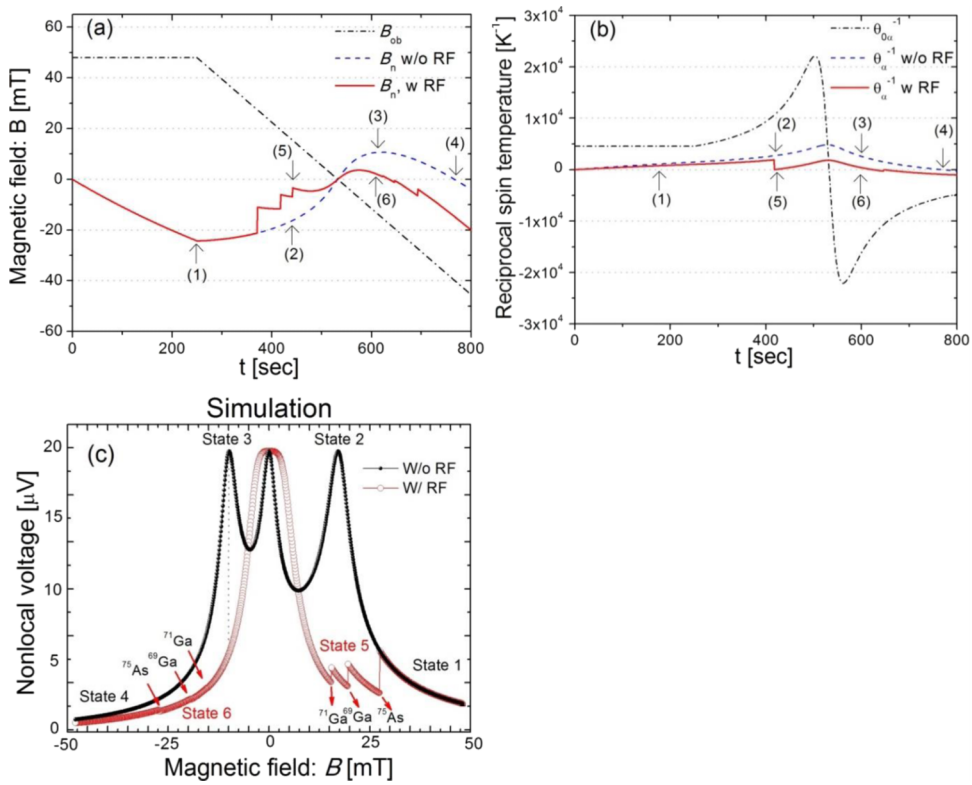

FIG. 4. Time evolution of (a) B_{ob} and B_n (with & without rf field), (b) $1/\theta_{0\alpha}$ and $1/\theta_\alpha$ for ^{75}As isotope in GaAs (with & without an rf field), and (c) simulation result for oblique Hanle signal (with & without an rf field).

Case 1: Analysis of the transient response of oblique Hanle effect measurement without NMR

Because $b_n^{(a)}$ is negative in GaAs, we know from eqs. (1) and (2) that if θ_a is positive (negative), $\mathbf{I_{av}}$ is parallel (antiparallel) to $\mathbf{B}_{ob}$, while $\mathbf{B_n}$ is antiparallel (parallel) to $\mathbf{B}_{ob}$. Thus, a condition that $\mathbf{B}_{ob}$ and $\mathbf{B_n}$ cancel each other exists only for $\theta_\alpha > 0$. Figure 4(a) shows $\mathbf{B}_{ob}$, $\mathbf{B}_n$ (*blue curve*) and (b) shows $1/\theta_{0\alpha}$ and $1/\theta_\alpha$ (*blue curve*) of ^{75}As nuclei as a function of time, while (c) shows a simulation result (*black curve*) for an oblique Hanle signal without NMR. We defined the nuclear field vector $\mathbf{B_n} = B_n(\mathbf{x}\sin\varphi + \mathbf{y}\cos\varphi)$. The value of θ_α^{-1} increased during a holding time due to DNP, resulting in the nuclear field $\mathbf{B_n}$ being generated antiparallel to $\mathbf{B}_{ob}$ at $t = t_{hold}$ [*state-1 in* Fig. 4(c) & Fig. 5(a)]. When B_{ob} reached 27 mT in the negative sweep direction, $\mathbf{B_n}$ and $\mathbf{B}_{ob}$ cancelled each other out, leading to one side peak in the nonlocal voltage V_{NL} [*state-2 in* Fig. 4(c) & Fig. 5(a)]. When $\mathbf{B}_{ob}$ was reversed, $\theta_{0\alpha}$ became negative because $\mathbf{B}_{ob}\cdot\mathbf{S} < 0$. This means $\mathbf{B}_{ob}$ and $\mathbf{B_n}$ should have been parallel and no cancellation should have occurred in the steady state [Fig. 5(b)]. However, a clear peak appeared also for negative $\theta_{0\alpha}$, exactly at $B_{ob} = -11$ mT, indicating a possible cancellation between $\mathbf{B}_{ob}$ and $\mathbf{B_n}$. According to our model, when $\mathbf{B_{ob}}$ was changed before the nuclear spin system reached the steady-state, θ_α^{-1} was delayed with respect to $\theta_{0\alpha}^{-1}$ as shown in Fig. 4(b), hence θ_α stayed positive for a certain time after $\mathbf{B}_{ob}$ was reversed. This time there was a delay because the external magnetic field was changed much faster than the T_1 and T_{1e} processes. After $\mathbf{B}_{ob}$ was reversed, the nuclear spin system adiabatically changed their spin direction to keep the Zeeman energy in the lower energy state for the negative B_{ob} as for the positive B_{ob}. As a consequence, $\mathbf{B_n}$ was generated antiparallel to $\mathbf{B}_{ob}$. The cancellation condition might then be satisfied. This gives rise to a possibility that the nuclear spin polarization can occur; i.e., $\theta_\alpha > 0$ although $\mathbf{B}_{ob}\cdot\mathbf{S} < 0$, [*state-3 in* Fig. 4(c) & Fig. 5(c)]. Thus, this case cannot be explained by $\theta_{0\alpha}$ and only reproduced by the transient response of θ_α. However, after sufficient time – that is, at $t > 650$ s – a state of population inversion of nuclear spins happened due to the DNP process and θ_α became negative, indicating $\mathbf{B_n}$ was parallel to $\mathbf{B}_{ob}$ [*state-4 in* Fig. 4(c) & Fig. 5(b)]. Therefore, no cancellation between $\mathbf{B}_{ob}$ and $\mathbf{B_n}$ would have occurred, resulting in the disappearance of the satellite peak.

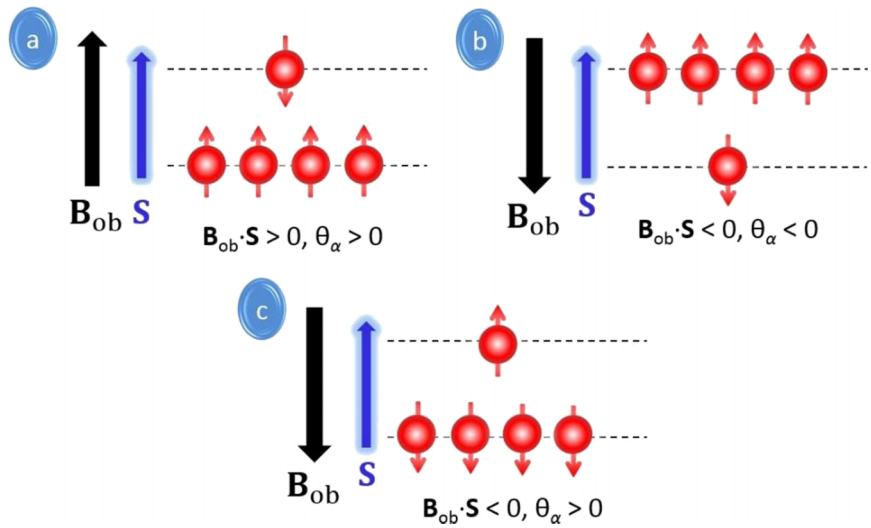

FIG. 5. Schematic description for nuclear spin distribution during sweeping of B_{ob} without NMR: (a) state-1 and state-2, (b) state-4, and (c) state-3. If B_{ob} is swept slowly enough for nuclear spins to reach the steady state, nuclear spin distribution changes from (a) to (b). However, if B_{ob} is swept faster than the time scale of T_{1e}, the distribution changes from (a) to (b) through the (c) state.

Case 2: Analysis of the transient response of oblique Hanle effect measurement with NMR

Figure 4(a) shows B_{ob} (*black curve*), B_n (*red curve*) and (b) shows $1/\theta_{0\alpha}$ (*black curve*) and $1/\theta_\alpha$ (*red curve*) of ^{75}As nuclei as a function of time, while (c) shows a simulation result (*red curve*) for an oblique Hanle signal with NMR, where B_n is the amplitude of $\mathbf{B_n}$ with both positive and negative signs; i.e., $\mathbf{B_n} = B_n(\mathbf{x}\sin\varphi + \mathbf{z}\cos\varphi)$. It is obvious that there is a great difference between the transient oblique Hanle signal before and after irradiation by the rf field. For instance, at $B_{ob} > 0$, the significant peak corresponding to the nuclear spin polarization was changed to a step-dip structure at $B_{ob} = 30.6, 22.0$, and 17.6 mT; those fields are equivalent to the resonant fields of ^{75}As, ^{69}Ga and ^{71}Ga, respectively. Moreover, for $B_{ob} < 0$, the transient state of nuclear spin polarization disappeared. These behaviors can be explained as follows. Due to DNP for $B_{ob} > 0$; a predicted situation similar to that one without irradiation by an rf field is dominant; i.e., $\theta_\alpha > 0$. This leads to the generation of a nuclear field $\mathbf{B_n}$ antiparallel to $\mathbf{B}_{ob}$ [*state-1 in* Fig. 4(c) & Fig. 5(a)]. Thereafter, nuclear spin polarization should be enhanced in a similar sense to [*state-2 in* Fig. 4(c) & Fig. 5(a)]; however irradiation by an rf field with an energy equal to the Zeeman splitting energy leads to the transition of nuclear spins between the ground state and the higher excited state, resulting in the disappearance of nuclear spin polarization because of dephasing [*state-5 in* Fig. 4(c) & Fig. 1(d)]. This means that the nuclear spin temperature is going to infinity. Thus, NMR acts as a heating tool for the nuclear spins.

Remarkably, there is a significant difference between the transient behaviors of ${\theta_\alpha}^{-1}$ for the oblique Hanle signal without NMR (*case 1*) and with NMR (*case 2*). This can be explained as follows. For case 1, the positive ${\theta_\alpha}^{-1}$ can travel over $B_{ob} = 0$ passing to $B_{ob} < 0$, and standing for a certain time under the influence of DNP only, produce a non-equal zero for B_n across this pass. For case 2, however, the positive ${\theta_\alpha}^{-1}$ was reset to zero when the NMR was done; i.e., $B_n = 0$. Then, it gradually cooled. But the strength of B_n weakly recovered from the situation of magnetic resonance ($B_n = 0$). Therefore, for case 2, after reversing the direction of $\mathbf{B}_{ob}$, ${\theta_\alpha}^{-1}$ is a positive value but smaller than that for case 1. Correspondingly, the generated nuclear Overhauser field was too weak [*state-6 in* Fig. 4(c)], giving rise to no nuclear spin polarization peak that could be detected for the change of the nonlocal voltage. Equally important, the resonance condition might be satisfied also for $B_{ob} < 0$ at $B_{ob} = -30.6, -22.0$, and -17.6 mT. Nevertheless, the corresponding step-dip signal was also too weak to be observable in contrast to that for $B_{ob} > 0$. Although we observed a small dip at $B_{ob} = -10$ mT in the experimental oblique Hanle signal with irradiation by an rf field, this was not due to the NMR; possibly it was due to environmental noise during the measurement, because $B_{ob} = -10$ mT is outside of the resonant condition. After a sufficient time – that is, at $t > 650$ s – there was a population inversion of nuclear

spins because DNP became dominant again and θ_α^{-1} became negative, indicating $\mathbf{B_n}$ was parallel to $\mathbf{B}_{ob}$ in a similar way to [*state-4 in* Fig. 4(c)].

IV. CONCLUSIONS

The transient response of nuclear spins with respect to the sweep of an external magnetic field in GaAs was well reproduced based on an interpretation between the steady state nuclear spin temperature and the time dependent transient state one. The analysis was introduced through a comparative study between oblique Hanle signals for the case with and without irradiation by an rf field. For the case without irradiation by an rf field, the analysis showed that the transient state of nuclear spins can be understood through the delay of time response of nuclear spin temperature to a change in the magnetic field. For the second case, when irradiation by an rf field with an energy equal to the Zeeman splitting energy is applied to the system, nuclear magnetic resonance occurs and the nuclear spin temperature exceeds the lattice temperature. One can therefore conclude that the dynamical nuclear polarization acts as a cooling tool for the nuclear spins temperature whereas nuclear magnetic resonance acts as a heating tool up to a temperature higher than the lattice temperature. These analyses provide a quantitative understanding of nuclear spin dynamics in semiconductors for future computation processing.

ACKNOWLEDGMENT

This work was partly supported by Grants-in-Aid for Scientific Research (KAKENHI Grants No. 25286039 and 15K13960) from the Japan Society for the Promotion of Science (JSPS).

[1] T. Uemura, T. Akiho, Y. Ebina, and M. Yamamoto, Phys. Rev. B. **91**, 140410(R) (2015).
[2] M. I. Dyakonov, V. I. Perel, V. L. Berkovits, and V. I. Safarov, Sov. Phys. JETP **40**, 950 (1975).
[3] D. Paget, G. Lampel, B. Sapoval, and V. I. Safarov, Phys. Rev. B **15**, 5780 (1977).
[4] G. Lampel, Phys. Rev. Lett. **20**, 491 (1968).
[5] J. Strand, B. D. Schultz, A. F. Isakovic, C. J. Palmstrøm, and P. A. Crowell, Phys. Rev. Lett. **91**, 036602 (2003).
[6] D. Gammon, S. W. Brown, E. S. Snow, T. A. Kennedy, D. S. Katzer, and D. Park, Science **277**, 85 (1997).
[7] G. Salis, D. T. Fuchs, J. M. Kikkawa, and D. D. Awschalom, Phys. Rev. Lett. **86**, 2677 (2001).
[8] T. Machida, T. Yamazaki, and S. Komiyama, Appl. Phys. Lett. **80**, 4178 (2002).
[9] K. Hashimoto, K. Muraki, T. Saku, and Y. Hirayama, Phys. Rev. Lett. **88**, 176601 (2002).
[10] M. Poggio, G.M. Steeves, R. C. Myers, Y. Kato, A. C. Gossard, and D. D. Awschalom, Phys. Rev. Lett. **91**, 207602 (2003).
[11] K. Ono and S. Tarucha, Phys. Rev. Lett. **92**, 256803 (2004).
[12] J. Strand, X. Lou, C. Adelmann, B. D. Schultz, A. F. Isakovic, C. J. Palmstrøm, and P. A. Crowell, Phys. Rev. B **72**, 155308 (2005).
[13] P. Van Dorpe, W. Van Roy, J. De Boeck, and G. Borghs, Phys. Rev. B **72**, 035315 (2005).
[14] M. K. Chan, Q. O. Hu, J. Zhang, T. Kondo, C. J. Palmstrøm, and P. A. Crowell, Phys. Rev. B **80**, 161206(R) (2009).
[15] G. Salis, A. Fuhrer, and S. F. Alvarado, Phys. Rev. B **80**, 115332(R) (2009).
[16] J. Shiogai, M. Ciorga, M. Utz, D. Schuh, T. Arakawa, M. Kohda, K. Kobayashi, T. Ono, W. Wegscheider, D. Weiss, and J. Nitta, Appl. Phys. Lett. **101**, 212402 (2012).
[17] T. Akiho, J. Shan, H.-x. Liu, K.-i. Matsuda, M. Yamamoto, and T. Uemura, Phys. Rev. B. **87**, 235205 (2013).
[18] H.-x. Liu, Y. Honda, T. Taira, K.-i. Matsuda, M. Arita, T. Uemura, and M. Yamamoto, Appl. Phys. Lett. **101**, 132418 (2012).
[19] H.-x. Liu, T. Kawami, K. Moges, T. Uemura, M. Yamamoto, F. Shi, and P. M. Voyles, J. Phys. D: Applied Physics **48**, 164001 (2015).
[20] M. Yamamoto, T. Ishikawa, T. Taira, G.-f. Li, K.-i. Matsuda, and T. Uemura, J. Phys.: Condens. Matter **22**, 164212 (2010).
[21] G.-f. Li, Y. Honda, H.-x. Liu, K.-i. Matsuda, M. Arita, T. Uemura, M. Yamamoto, Y. Mimura, M. Shirai, T. Saito, F. Shi, and P. M. Voyles, Phys. Rev. B **89**, 014428 (2014).
[22] J.-P. Wüstenberg, R. Fetzer, M. Aeschlimann, M. Cinchetti, J. Minár, Jürgen Braun, H. Ebert, T. Ishikawa, T. Uemura, and M. Yamamoto, Phys. Rev. B **85**, 064407 (2012).
[23] V. R. Singh, V. K. Verma, K. Ishigami, G. Shibata, T. Kadono, A. Fujimori, D. Asakura, T. Koide, Y. Miura, M. Shirai, G.-f. Li, T. Taira, and M. Yamamoto, Phys. Rev. B **86**, 144412 (2012).
[24] Y. Ebina, T. Akiho, H.-x. Liu, M. Yamamoto, and T. Uemura, Appl. Phys. Lett. **104**, 172405 (2014).
[25] A. Abragam and W. G. Proctor, Spin Temperature. Phys. Rev **109**, 1441 (1958).
[26] M. I. Dyakonov and V. I. Perel, in *Optical Orientation*, edited by F. Meier and B. P. Zakharchenya (North-Holland, New York, 1984).
[27] X. Lou, C. Adelmann, S. A. Crooker, E. S. Garlid, J. Zhang, S. M. Reddy, S. D. Flexner, C. J. Palmstrøm, and P. A. Crowell, Nat. Phys. **3**, 197 (2007).
[28] G. Salis, A. Fuhrer, R. R. Schlittler, L. Gross, and S. F. Alvarado, Phys. Rev. B **81**, 205323 (2010).
[29] M. Ciorga, A. Einwanger, U. Wurstbauer, D. Schuh, W. Wegscheider, and D. Weiss, Phys. Rev. B **79**, 165321 (2009).
[30] J. Fabian, A. Matos-Abiaguea, C. Ertlera, P. Stano, and I. I. Zutic, Acta Phys. Slov. **57**, 565 (2007).
[31] I. Zutic, J. Fabian, and S. D. Samra, Rev. Mod. Phys. **76**, 323 (2004).